New J. Chem., 1996, **20**, 523-536

X-ray diffraction and solid state NMR studies of 1,8-bis(dimethylamino)naphthalene and its complexes with picric and hexafluorophosphoric acids

Concepción LÓPEZ and Rosa María CLARAMUNT*

Departamento de Química Orgánica y Biología, Facultad de Ciencias, UNED, Senda del Rey s/n, E-28040 Madrid, Spain.

Antonio L. LLAMAS-SAIZ and Concepción FOCES-FOCES*

Departamento de Cristalografía, Instituto de Química Física "Rocasolano", CSIC, Serrano 117, E-28006 Madrid, Spain.

José ELGUERO and Isabel SOBRADOS

Institutos de Química Médica y de Materiales, CSIC, Juan de la Cierva 3, E-28006 Madrid, Spain.

Francisco AGUILAR-PARRILLA and Hans-Heinrich LIMBACH

Institut für Organische Chemie (WE 02), Freie Universität Berlin, Takustraβe 3, D-14195 Berlin, Germany.

Received October 20, 1995, accepted November 11, 1995.

Abstract. – In order to get a better understanding of the nature of the N^+–H···N′ system characterizing the intramolecular hydrogen bond in classical proton sponges, crystal structure determinations at room temperature and at 150 K have been undertaken for the picrate and the hexafluorophosphate salts of 1,8-bis(dimethylamino)naphthalene (DMAN). Two polymorphic forms were detected for the picrate. The crystals of the orthorhombic form twinned when they were cooled. The elongated N^+–H distances, even at low temperature, are indicative of proton disorder. The polymorphism of DMAN picrate proved crucial in establishing the complementarity between the CPMAS NMR (^{13}C and ^{15}N) and crystallography results.

Introduction

In a review on "Proton Sponges" [1] we summarized all the structural information available on this class of compounds through the end of 1993. The discussion was mainly statistical and based on crystal structures including some unpublished results. In particular, the data on the PF_6^- and the picrate salts of 1,8-bis(dimethylamino)naphthalene (DMAN) were briefly commented (see ref. 58 in ref. 1). Since this review, some relevant papers have appeared. One by Szafran et al. [2] reported the ^{13}C NMR spectra of DMAN complexes with mineral acids in solution (anions: Cl^-, Br^-, NO_3^-, ClO_4^-, BF_4^-). Stefaniak et al. [3] described the ^{13}C and ^{15}N NMR spectra of two proton sponges, different from DMAN, in solution and in the solid state. Grech et al. [4] have published the X-ray structure of $DMANH^+$ SCN^- at 188 and 290 K. Platts, Howard and Wozniak [5] have carried out *ab initio* calculations on DMAN and $DMANH^+$.

In a recent publication, Wozniak et al. [6] reported an interesting observation. The X-ray structures, as well as the ^{13}C CPMAS NMR spectra of DMAN and two of its complexes (anions: BF_4^-, NCS^-), were described. For these salts, two methyl groups at 43.6 and 46.4 ppm (BF_4^-) and at 44.6 and 47.4 ppm (NCS^-) were observed. Since in DMAN, four methyl group signals are observed, the authors commented, without favoring one alternative over the other that the averaging in the salts may be caused by a flattering of the naphthalene ring or by a fast exchange of the trapped proton.

One of the aims of the present paper is to find out if the structural information obtained by crystallography is consistent with that coming from solid state NMR. This is a complex problem needing a careful discussion of the possible structures as well as several assumptions to reach some preliminary conclusions. In the following

discussion, the intramolecular hydrogen bond (IMHB) of the $DMANH^+$ cation will be represented in a simplified way:

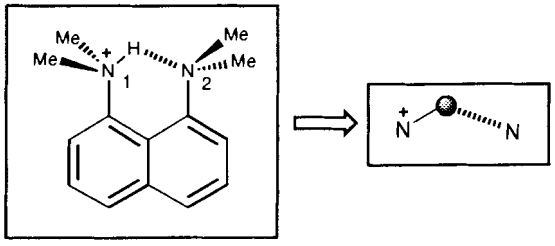

Crystallography

Let us assume that there is only one independent molecule in the unit cell. Three limiting situations are possible for the position of the $(NHN)^+$ proton (Scheme 1). **A** proton *located* on N(1) and hydrogen bonded to N(2), **B** proton *shared*, i.e., in the center of the IMHB, **C** proton *disordered* with populations (x) and $(1-x)$ on N(1) and N(2).

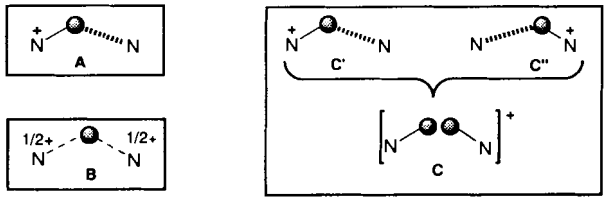

Scheme 1.

There is no ambiguity in cases **A** and **B**, the proton being clearly located. Case **C** is a superposition of cases **C′** [N(1)–H] and **C″** [N(2)–H]; since part of a proton is often difficult to locate in X-ray crystallography (even at low temperatures), case **C** will thus be experimentally observed only when the population (x) is near 0.5, i.e. when $K = [\mathbf{C}']/[\mathbf{C}''] \approx 1$. Case **C** could correspond either to a static disorder (some unit cells with molecules **C′** and some unit cells with molecules **C″**) or to a dynamic disorder (all unit cells containing molecules **C′** and **C″** with rapid or slow proton transfer). As Etter has commented for the related case of pyrazole trimers [7], lowering the temperature of $DMANH^+$ crystals having structure **C** will only result in transforming the dynamic disorder into a disordered static structure without any observable crystallographic difference.

The other cause of complexity arises from the position of the methyl groups with respect to the naphthalene plane. We have illustrated the **A** case (but it is identical for **B** and **C**) with situation **a** where the methyl groups are symmetrically placed with respect to the aromatic ring (torsions: 60°, −60°, 60°, −60°) and situation **b** where they are more or less rotated (Scheme 2). The perfect case **a** is only present when the molecule has some crystallographic symmetry elements.

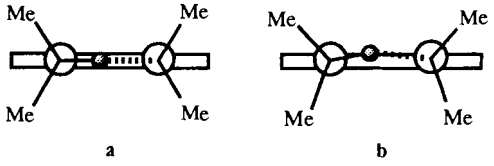

Scheme 2.

^{15}N CPMAS NMR

Let us continue to assume that there is only one independent molecule in the unit cell. Four different "observable" results are expected (but only if the chemical shift differences are large enough, would the number of lines correspond to the number of inequivalent N atoms), which are summarized in Scheme 3:

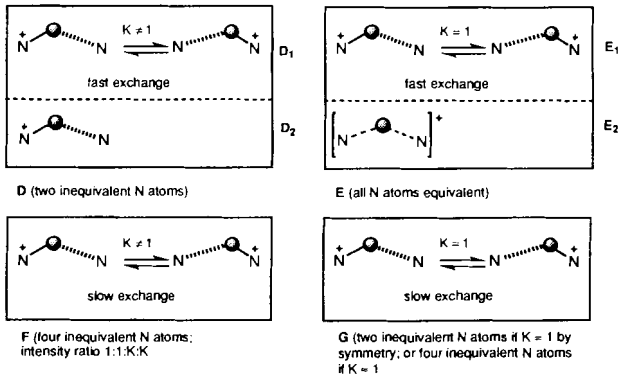

Scheme 3.

The position of the methyl groups (**a** or **b**) is irrelevant for the ^{15}N NMR results. Situations $\mathbf{D_1}$ *vs* $\mathbf{D_2}$ and $\mathbf{E_1}$ *vs* $\mathbf{E_2}$ are indistinguishable by NMR chemical shifts.

^{13}C CPMAS NMR

In this case, it is necessary to add the position of the methyl groups to the **D-G** possibilities in Scheme 3, resulting in the following classes: **Da** 2 inequivalent Me groups, **Db** 4 inequivalent Me groups, **Ea** all methyl equivalent, **Eb** 2 inequivalent Me groups, **Fa** 2 inequivalent Me groups, **Fb** 4 inequivalent Me groups, **Ga** 2 inequivalent Me groups, and **Gb** 4 inequivalent Me groups.

In Table I are gathered the correspondences between the X-ray structures (**A** to **C**) and the number of NMR signals (**D** to **G**), remembering that (i) it is assumed that there is only one independent molecule in the unit cell and (ii) the number of lines (^{15}N, ^{13}C) corresponds to the number of inequivalent N or C atoms only if the chemical shifts difference are large enough.

Table I. – Relationship between crystallography and ^{13}C and ^{15}N CPMAS NMR.

X-ray structure	^{13}C NMR (Me groups)	^{15}N NMR
Aa	$\mathbf{D_2a}$ (2 Me)	$\mathbf{D_2}$ (2 N)
Ab	$\mathbf{D_2b}$ (4 Me)	$\mathbf{D_2}$ (2 N)
Ba	$\mathbf{E_2a}$ (1 Me)	$\mathbf{E_2}$ (1 N)
Bb	$\mathbf{E_2b}$ (2 Me)	$\mathbf{E_2}$ (1 N)
	$\mathbf{D_1a}$ (2 Me)	$\mathbf{D_1}$ (2 N)
Ca	$\mathbf{E_1a}$ (1 Me)	$\mathbf{E_1}$ (2 N)
	Fa (2 Me)	**F** (4 N)
	Ga (2 Me)	**G** (2 or 4 N)
	$\mathbf{D_1b}$ (4 Me)	$\mathbf{D_1}$ (2 N)
Cb	$\mathbf{E_1b}$ (2 Me)	$\mathbf{E_1}$ (1 N)
	Fb (4 Me)	**F** (4 N)
	Gb (4 Me)	**G** (2 or 4 N)

Experimental section

General methods

M.p.: hot-stage microscope; uncorrected. The high-resolution solid state ^{13}C NMR spectra were obtained at room temperature on a Bruker AC-200 spectrometer (UNED) operated at 50.32 MHz under cross polarization (CP) and magic angle spinning (MAS) conditions, using a 7-mm Bruker DAB 7 probehead that achieves rotational frequencies of about 3.5-4.5 kHz. Samples (approximately 200 mg of material) were carefully packed in ZrO_2 rotors. The standard CPMAS pulse sequence was applied with a 7 μs ^1H-90° pulse width, 3-5 ms contact pulses, and 5 s repetition time, the spectral width being 20 000 Hz. All chemical shifts are given with respect to the spectrometer reference frequency, which was calibrated by the glycine signal at 176.1 ppm. The ^{13}C CPMAS NMR spectra of hexafluorophosphate **1**, picrates **1I** and **1II** (see Fig. 1), tetrazolate **6** and perchlorate **9** were recorded on a Bruker MSL 400 instrument (for experimental conditions, see ref. 8); although there are minor differences, **qualitatively** both instruments yield the same spectra (the data in Table II are those of the MSL 400 spectrometer).

The ^{15}N CPMAS NMR spectra were recorded on a Bruker MSL 300 spectrometer (FU Berlin) operated at 300.13 MHz for protons and 30.41 MHz for ^{15}N. The spectrometer was equipped with a 5-mm high-speed CPMAS probehead from Doty Scientific, USA. A Bruker B VT 1000 temperature unit was used to control the temperature of the bearing nitrogen gas stream. The standard CPMAS pulse sequence was again applied here: 5 μs ^1H 90° pulse width, 4-12 ms CP time and 4 s recycle delay, spectral width of 15 000 Hz. All ^{15}N chemical shifts are related to external solid $^{15}NH_4Cl$; ppm values for narrow lines are given with an error of ±0.3 ppm, broad lines with ±0.5 ppm.

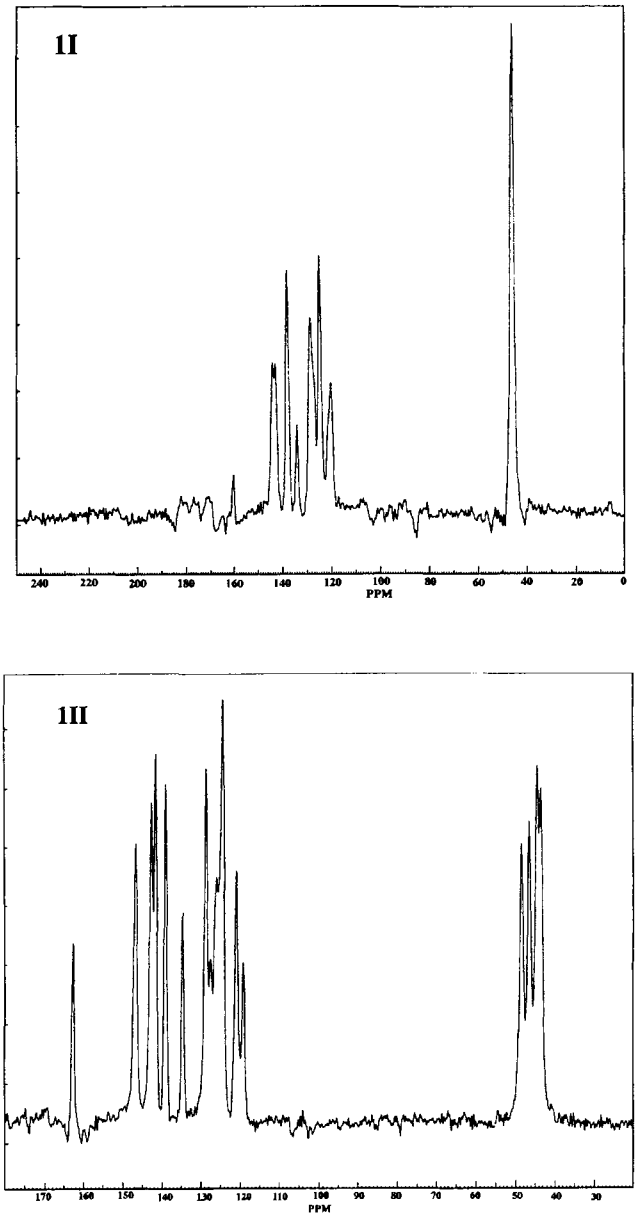

Figure 1. – ^{13}C CPMAS NMR spectra (100 MHz) of picrates **1I** and **1III**.

The salts were generally prepared by crystallization from an equimolar solution of DMAN and the corresponding acid in the appropriate solvent, usually acetonitrile. In the case of tetrafluoroborate, tetrazolate, bromide, pentachlorophenolate and squarate, literature procedures were followed [1]; the perchlorate **9** was prepared according to ref. 2. Picrates **1I** and **1III**: (i) To a solution of 500 mg of DMAN (2.33 mmol) in 5 mL CH_3CN was added 534 mg of picric acid (2.33 mmol) in 5 mL CH_3CN; at this concentration, the DMAN picrate is soluble in CH_3CN. If this solution is allowed to evaporate at RT (in a Petri dish), crystals of picrate (variety **1I**) appeared, under

Table II. – CPMAS NMR chemical shifts (ppm).

Anion	Me	^{13}C CPMAS NMR						^{15}N CPMAS NMR
		C_1, C_8	C_2, C_7	C_3, C_6	C_4, C_5	C_9	C_{10}	
Neutral DMAN [6]	41.0, 41.8, 44.2, 45.1			see ref. 6				4.1 [a]
Picrate **1** form **I**	46.0 [b]	143.0 144.1	120.0	124.7	128.5	120.0	134.2	−5.1 [c]
Picrate **1** form **II**	48.7, 46.7, 44.7, 43.8 [d]	141.6 142.7 146.7	120.9	124.5 127.4	128.7	119.2	134.6	−5.6 [e] −2.1 3.6
PF_6^- **2**	43.0, 45.8	143.3	120.0	126.0	127.6	117.0	134.4	−5.4
$C_6Cl_5O^-$ **3**	45.6, 47.9, 49.9 (1:1:2)	143.0 144.3 145.4	118.7	124.3 126.8	127.4	118.7	135.6	−3.4, −5.7
Squarate **4**	46.1	145.1	123.6	125.5	128.7	117.7	136.0	−4.7 [f]
Tetrazolate **6** [11]	44.7	145.2 [g]	124.3 [g]	128.7 [g]	131.2 [g]	117.8 [g]	136.2	[h]
Tetrazolate **6** [i]	44.2	144.7	123.6	128.0	130.6	116.7	135.4	−6.3 [j]
BF_4^- **7** [6]	43.6, 46.4	143.4 [k]	120.7	126.5	128.3	117.4 [k]	134.8	–
BF_4^- **7**	43.8, 46.3	143.5	120.5	127.4	127.4	117.4	135.0	−5.1
SCN^- **8** [6]	44.8, 47.4	143.9 [k]	121.3	126.1	128.9	118.1 [k]	134.6	–
ClO_4^- **9**	43.6, 46.5	143.1	120.4	126.6	128.0	117.0	134.5	−4.7

[a] $\delta(^{15}N) = -329.7$ ppm (ref. neat nitromethane) [11] [338.1 − 329.7 = 8.4 ppm (ref. solid $^{15}NH_4Cl$)]; $\delta(^{15}N) = -336.9$ ppm (ref. neat nitromethane) [10] [338.1 − 336.9 = 1.2 ppm (ref. solid $^{15}NH_4Cl$)]. [b] Picrate anion: 160.4 ($C_{1'}$), 138.1 ($C_{2'}$, $C_{6'}$), 124.7 ($C_{3'}$, $C_{4'}$, $C_{5'}$). [c] Picrate anion: 327.3, 328.6 ppm (*ortho*-NO_2). [d] Picrate anion: 162.5 ($C_{1'}$), 139.0 ($C_{2'}$, $C_{6'}$), 126.0 ($C_{3'}$, $C_{5'}$), 124.5 ($C_{4'}$). [e] Picrate anion: 327.3, 329.6 (*ortho*-NO_2). [f] $\delta(^{15}N) = -346.0$ ppm (ref. neat nitromethane) [10] [338.1 − 346.0 = −7.9 ppm (ref. solid $^{15}NH_4Cl$)]. [g] These signals were incorrectly assigned in ref. 11, in particular, the signals of C_1,C_8 (145.2 ppm) and the tetrazolate carbon (151.0 ppm) were inverted. [h] $\delta(^{15}N) = -340.0$ ppm (ref. neat nitromethane) [11] [338.1 − 340.0 = −1.9 ppm (ref. solid $^{15}NH_4Cl$)]. [i] Tetrazolate anion, $\delta(^{13}C) = 151.0$ ppm. [j] Tetrazolate anion: 277.5 ($N_{1'}$), 346.6 ppm ($N_{2'}$) (see refs. 11, 16 for the assignment of tetrazole nitrogen atoms), $\delta(^{15}N) = -56.4$ ($N_{1'}$), +11.4 ($N_{2'}$) ppm (ref. neat nitromethane) [11] [338.1 − 56.4 = 281.7; 338.1 + 11.4 = 349.5 ppm (ref. solid $^{15}NH_4Cl$)]. [k] Reversed assignment [6].

microscope the crystals show modifications near 155 °C and finally melt at 164-6 °C. Anal calc for $C_{20}H_{21}N_5O_7$ (443.41): C 54.17, H 4.77, N 13.20; found: C 54.44, H 4.77, N 15.72. (ii) To a solution of 500 mg of DMAN (2.33 mmol) in 10 mL EtOH was added 534 mg of picric acid (2.33 mmol) in 10 mL EtOH, long needles of picrate **1II** appear immediately, m.p. 164-6 °C. Anal calc for $C_{20}H_{21}N_5O_7$ (443.41): C 54.17, H 4.77, N 13.20; found: C 54.31, H 4.81, N 15.63. The hexafluorophosphate **2** was obtained from an equimolar ethanol solution, m.p. 280-2 °C. Anal calc for $C_{14}H_{19}N_2PF_6$ (360.66): C 46.62, H 5.41, N 7.77; found: C 46.71, H 5.32, N 7.84.

^{13}C NMR spectroscopy in solution (δ in ppm; ^{1}H-^{13}C coupling constants in Hz). Picric acid ([$^2H_6$]DMSO) 159.7 ($C_{1'}$), 141.9 ($C_{2'}$, $C_{6'}$), 125.8 ($C_{3'}$, $C_{5'}$), 127.2 ($C_{4'}$). Sodium picrate ([$^2H_6$]DMSO) 161.0 ($C_{1'}$), 141.8 ($C_{2'}$, $C_{6'}$), 125.4 ($C_{3'}$, $C_{5'}$), 124.5 ($C_{4'}$). DMAN (CD_3OD) 45.15 (4 methyl groups, $^1J = 134.3$, $^3J = 4.4$), 122.17 (C_9, $^3J = 5.7$), 114.09 (C_2, C_7, $^1J = 157.9$, $^3J = 8.1$), 126.65 (C_3, C_6, $^1J = 159.5$), 123.18 (C_4, C_5, $^1J = 160.3$, $^3J = 7.5$, $^3J = 5.1$), 139.46 (C_{10}, m), 152.05 (C_1, C_8, $^3J = 6.2$, $^3J = 3.2$). Hexafluorophosphate **2** (CD_3CN), 46.67 (4 methyl groups, $^1J = 140.8$, $^3J = 4.0$), 120.16 (C_9, m), 122.54 (C_2, C_7, $^1J = 161.0$, $^3J = 8.7$), 128.05 (C_3, C_6, $^1J = 166.6$), 130.22 (C_4, C_5, $^1J = 164.8$, $^3J = 7.0$, $^3J = 5.6$), 136.54 (C_{10}, $^2J = 2.5$, $^3J = 8.5$), 145.33 (C_1, C_8, m). Picrate **1** (CD_3CN, forms **I** and **II** yield identical spectra): 45.72 (4 methyl groups), 117.30 (C_9), 121.50 (C_2, C_7), 125.41 (picrate $C_{3'}$, $C_{5'}$), 126.98 (C_3, C_6), 129.17 (C_4, C_5), 135.50 (C_{10}), 144.23 (C_1, C_8). This assignment of $DMANH^+$ carbon-13 chemical shifts (based on coupling constants) is consistent with our assignment for related pyrimidines [9], and with those of Szafran [2] and of older work by Grech [10], but reverses the assignments of C_9 *vs* C_1-C_8 in a recent publication by Grech [6].

^{15}N NMR spectroscopy in solution (δ in ppm from external nitromethane; ^{1}H-^{15}N coupling constants in Hz). In contrast to ^{13}C NMR spectroscopy, where TMS is the universally accepted reference, there is not a universal reference of ^{15}N NMR spectroscopy. Nitromethane has been accepted for solution studies but it is unsuitable for solid state studies. Some authors [10, 11] used neat nitromethane for ^{15}N CPMAS chemical shifts, but although these shifts can be converted into the solid $^{15}NH_4Cl$ reference using $\delta CH_3NO_2 + 338.1$ ppm (355.3 ppm from CH_3NO_2 to saturated $^{15}NH_4Cl$-D_2O and −17.2 ppm from saturated $^{15}NH_4Cl$-D_2O to solid $^{15}NH_4Cl$) [12, 13], they are not directly comparable because they have been calculated using an approximate relationship between chemical shift references [14, 15]. Picrate sodium salt ([$^2H_6$]DMSO) −11.1 [d, ^3J (^{1}H-^{15}N) = 3.0 Hz], −14.6 [t, ^3J (^{1}H-^{15}N) = 1.8 Hz]; conversion to solid ammonium chloride ($\delta CH_3NO_2 + 338.1$ ppm [12]) yields *ortho*-NO_2 327.0 and *para*-NO_2 (difficult to observe) 323.5 ppm.

The CPMAS NMR results are gathered in Table II. The numbering system, as used in other publications on NMR of proton sponges, differs from that used in crystallography (carbons C_9 and C_{10} should be renamed C_{8a} and C_{4a}).

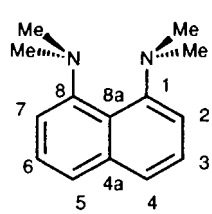

X-ray crystal-structure determination

The picrate compound, **1**, crystallizes in an orthorhombic cell, form **I**, with four molecules in the unit cell, so that both ions are located in mirror planes. It also crystallizes in a monoclinic cell, form **II**. Data were collected at room temperature and at 150 K except in form **I**; in this last case, the crystals twin when cooling in a reversible process. The crystals were cooled utilizing an Oxford Cryostream device and the temperature was measured continuously during data collections, showing fluctuations of ±0.1°. The same crystal was used for the picrate compound, form **II**, and two different ones for the PF_6^- salt, compound **2**, since they split if the temperature is not decreased slowly. The experimental details and the most relevant refinement parameters are given in Tables IIIa and IIIb. The structures were solved by direct methods, SIR92 [17]. In the case of the PF_6^- salt, the empirical absorption correction was applied [18]. The non-hydrogen atoms were refined anisotropically and the hydrogen ones were included as isotropic. Ten and two reflections for compound **1**, both forms, were affected by secondary extinction and were considered as unobserved in the last refinement cycles. Most of the calculations were performed on a VAX6410 computer using the XRAY80 System [19]. The atomic coordinates are listed in Tables IV-VIII. The atomic scattering factors were taken from the *International Tables for X-Ray Crystallography*, Vol. IV [20].

Results and discussion

X-ray analysis

To get a better understanding of the nature of the N^+–H···N system involved in the intramolecular hydrogen bond of proton sponges, the crystal and molecular structures of the picrate **1** and PF_6^- **2** salts of $DMANH^+$ have been determined at room temperature and at 150 K (RT and LT hereafter) except for the polymorphic form **I** of the picrate (see *Experimental section*). The picrate exhibits polymorphism and two kinds of crystals are obtained depending on the solvent used for the crystallization: form **I** in acetonitrile and form **II** in ethanol; the crystals of salt **2** were obtained from an ethanol solution.

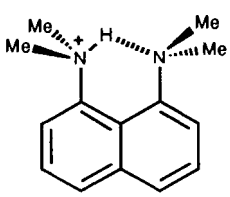

$DMANH^+$

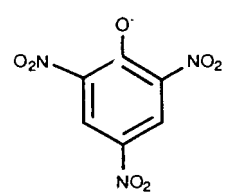

Picrate **1**

PF_6^-

2

Two perspective views of the molecular structures of compounds **1** (form **II**) and **2** at LT, with the numbering system used in crystallography are shown in Figure 2 [21]. Tables IXa and IXb display the most relevant geometric aspects. In form **I** of compound **1** both ions lie in the crystallographic symmetry planes. For polymorph **II** of compound **1** and for compound **2**, only data at low

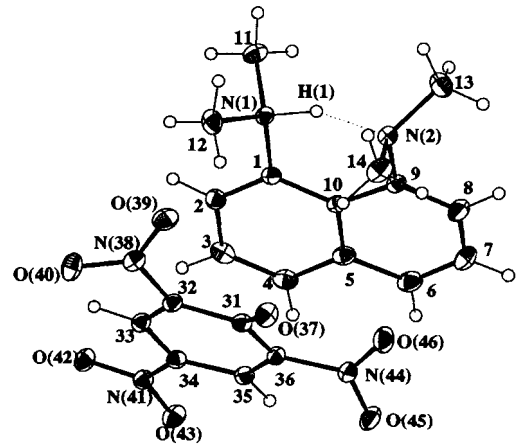

(a)

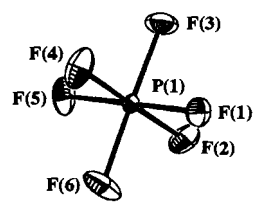

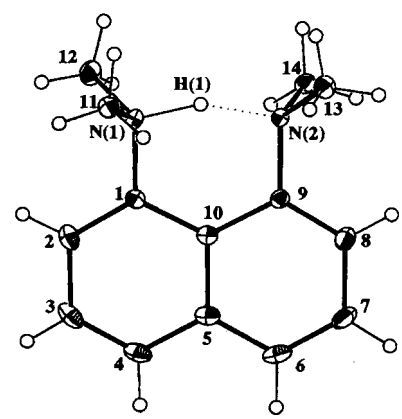

(b)

Figure 2. – (a) An ortep [21] view of form **III** at low temperature showing the numbering system. (b) Same for **2**. Ellipsoids are drawn at the 30% probability level. Dotted lines indicate hydrogen bonds.

temperature are retained since its isomorphism has been checked by means of half normal probability plots [22] using interatomic distances including those involving the torsion angles of the molecules. The main differences in compound **1** have been found between the N(1)···N(2), C(3)–C(4), C(6)–C(7) and C(7)–C(8) distances. In compound **2** the differences are due to the elongation of the P–F distances in the PF_6^- anion. They show values in the 1.545(7)-1.572(6) Å and 1.576(3)-

Table IIIa. – Crystal analysis parameters.

	1:Form **I**	**1**:Form **II**, RT	**1**:Form **II**, LT
Crystal data			
Formula	$C_{14}H_{19}N_2^+.C_6H_2N_3O_7^-$	$C_{14}H_{19}N_2^+.C_6H_2N_3O_7^-$	$C_{14}H_{19}N_2^+.C_6H_2N_3O_7^-$
Crystal habit	Yellow, prism	Yellow, octahedral	Yellow, octahedral
Crystal size (mm)	0.56 × 0.40 × 0.40	0.37 × 0.20 × 0.20	0.37 × 0.20 × 0.20
Symmetry	Orthorhombic, *Pnam*	Monoclinic, $P2_1/n$	Monoclinic, $P2_1/n$
Unit cell determination:	Least-squares fit from 70 reflexions ($\theta < 45°$)	Least-squares fit from 79 reflexions ($\theta < 45°$)	Least-squares fit from 84 reflexions ($\theta < 45°$)
Unit cell dimensions (Å, °)	$a = 16.2229(7)$	$a = 22.2163(15)$	$a = 22.1420(15)$
	$b = 18.2120(11)$	$b = 9.4961(4)$	$b = 9.4790(3)$
	$c = 6.9637(3)$	$c = 9.9584(4)$	$c = 9.7889(3)$
	90, 90, 90	90, 98.859(5), 90	90, 99.539(4), 90
Packing: V(Å^3), Z	2057.4(2), 4	2075.8(2), 4	2026.1(2), 4
Dc (g/cm^3), M, F(000)	1.432, 443.42, 928	1.419, 443.42, 928	1.454, 443.42, 928
μ (cm^{-1})	8.90	8.82	9.04
Experimental data			
Technique	Four circle diffractometer. Bisecting geometry. Graphite oriented monochromator. $\omega/2\theta$ scans. Detector apertures 1 × 1°. 1 min./reflex. Cu$K\alpha$ radiation.		
	Seifert XRD3000-S	Philips PW1100	Philips PW1100
Scan width:	1.5°	1.5°	1.5°
θ_{max}	67°	65°	65°
T (K)	295	295	150
Number of reflections:			
Independent	1928	3528	3440
Observed	1165 (3 σ (I) criterion)	2720 (3 σ (I) criterion)	2970 (3 σ (I) criterion)
Standard reflections:			
2 reflections every:	100	90	90 min
	No variation	No variation	No variation
Solution and refinement			
Solution		Direct methods: Sir92	
Refinement:			
Least-squares on F_0		Full matrix	
Parameters:			
Number of variables	238	373	373
Degrees of freedom	927	2347	2597
Ratio of freedom	4.9	7.3	8.0
Final shift/error	0.08	0.05	0.09
H atoms		From difference synthesis	
Weighting-scheme	Empirical as to give no trends in $\langle \omega \Delta^2 F \rangle$ vs $\langle \lvert F_{obs} \rvert \rangle$ and $\langle \sin\theta/\lambda \rangle$		
Max. thermal value (Å^2)	U33[O(40)] = 0.231(6)	U22[C(12)] = 0.126(4)	U22[C(13)] = 0.051(2)
Final ΔF peaks (eÅ^{-3})	0.25	0.29	0.24
Final R and Rw	0.058, 0.066	0.059, 0.071	0.049,0.056

1.597(2) Å ranges at RT and at LT respectively. The differences can be ascribed to the reduction of thermal vibration when decreasing the temperature. The question as to whether the elongation is related to some disordering will be discussed in the NMR section.

The DMAN skeleton is sensitive to protonation, mainly in the Me_2–N(1)–C(1)-C(10)–C(9)–N(2)–Me_2 region displaying N–C–C external angles greater than the N–C–C internal ones (Table IXa), in good agreement with the averaged reported values [1]. The naphthalene moiety is not planar, except in **1** form **I**, showing distortion values about the C(5)–C(10) bond, χ_T [23], of −5.1(1) and 3.7(2)° for form **II** and the PF_6^- salts, respectively, at low temperature. These values are greater than the average reported one of 1.7° (ref. 1).

In both forms of compound **1**, the bond lengths in the picrate anion are significantly elongated or shortened as compared with the standard C–C bond in the

Table IIIb. – Crystal analysis parameters.

	2, RT	**2, LT**
Crystal data		
Formula	$C_{14}H_{19}N_2^+.PF_6^-$	$C_{14}H_{19}N_2^+.PF_6^-$
Crystal habit	Colorless, plate	Colorless, plate
Crystal size (mm)	0.50 × 0.33 × 0.05	0.67 × 0.33 × 0.20
Symmetry	Triclinic, *P*-1	Triclinic, *P*-1
Unit cell determination:	Least-squares fit from 65 reflexions ($\theta < 45°$)	Least-squares fit from 70 reflexions ($\theta < 45°$)
Unit cell dimensions, (Å, °)	$a = 12.6273(16)$ $b = 8.2708(6)$ $c = 8.4699(4)$ 79.815(6), 107.155(7), 96.671(9)	$a = 12.4150(16)$ $b = 8.1173(6)$ $c = 8.4706(11)$ 80.020(8), 106.415(6), 98.170(11)
Packing: V(Å^3), Z	830.0(1), 2	802.5(2), 2
Dc (g/cm^3), M, F(000)	1.442, 360.28, 372	1.491, 360.28, 372
μ (cm^{-1})	20.52	21.23
Experimental data		
Technique	Four circle diffractometer. Bisecting geometry. Graphite oriented monochromator. $\omega/2\theta$ scans. Detector apertures 1 × 1°. 1 min./reflex. Cu$K\alpha$ radiation.	
	Seifert XRD3000-S	Philips PW1100
Scan width:	1.5	1.5°
θ_{max}	65°	65°
T (K)	295	150
Number of reflections:		
Independent	2848	2687
Observed	1585 (3 σ (I) criterion)	2475 (3 σ (I) criterion)
Standard reflections:		
2 reflections every:	90	90 min
	No variation	No variation
Solution and refinement		
Solution	Direct methods: Sir92	
Refinement:		
Least-squares on F_0	Full matrix	
Parameters:		
Number of variables	284	284
Degrees of freedom	1301	2191
Ratio of freedom	5.6	8.7
Final shift/error	0.02	0.01
H atoms	From difference synthesis	
Weighting-scheme	Empirical as to give no trends in $\langle \omega \Delta^2 F \rangle$ vs $\langle \lvert F_{obs} \rvert \rangle$ and $\langle \sin\theta/\lambda \rangle$	
Max. thermal value (Å^2)	U11[F(5)] = 0.192(6)	U11[F(4)] = 0.089(2)
Final ΔF peaks (eÅ^{-3})	0.46	0.81 near the P atom
Final R and Rw	0.065, 0.074	0.067, 0.086

benzene ring. The double bonds are mainly located at the C(31)–O(37), C(32)–C(33) and C(35)–C(36) bonds while the C–C bonds involving C(31) show single bond character. The C(34)–N(41) bond is also significantly shorter than the two other C–N bonds, indicating the predominance of the resonance form where the *para* nitro group is involved in the charge conjugation. In addition, this nitro group is almost coplanar with the six-membered ring in form **II**.

The internal angles reflect the influence of substituents (Table IXb), displaying values as low as 110° at C(31). The external angles are affected by the conformation of the nitro groups so that the greater the C–C–N–O torsion angle, the lower the angular distortion; values up to 5.0° are present in form **I** due to the fact that all atoms lie in a mirror plane.

As far as the IMHB is concerned, the N···N distances of compounds **II**, **III** and **2** (Table IXa, X···Y) are shorter than the average distance of 2.590(23) Å (standard deviation in parentheses) reported for the 25 DMANH$^+$ structures studied so far. However, the N$^+$–H bond is rather elongated and in the PF_6^- salt this value remains

Table IV. – Final atomic coordinates for **1**, Form **I**.

Atom	x	y	z
N(1)	0.4551(2)	0.1371(2)	0.2500
N(2)	0.3750(2)	0.2585(2)	0.2500
C(1)	0.3767(3)	0.0969(2)	0.2500
C(2)	0.3753(3)	0.0223(2)	0.2500
C(3)	0.3005(3)	-0.0167(2)	0.2500
C(4)	0.2286(3)	0.0203(2)	0.2500
C(5)	0.2268(3)	0.0980(2)	0.2500
C(6)	0.1511(3)	0.1363(3)	0.2500
C(7)	0.1492(3)	0.2105(3)	0.2500
C(8)	0.2229(3)	0.2512(3)	0.2500
C(9)	0.2974(2)	0.2165(2)	0.2500
C(10)	0.3024(2)	0.1386(2)	0.2500
C(11)	0.5029(2)	0.1231(2)	0.4279(6)
C(13)	0.3852(3)	0.3032(2)	0.4263(6)
C(31)	0.2628(2)	0.1391(2)	0.7500
C(32)	0.1840(2)	0.1790(2)	0.7500
C(33)	0.1086(3)	0.1466(2)	0.7500
C(34)	0.1032(3)	0.0705(2)	0.7500
C(35)	0.1734(3)	0.0275(2)	0.7500
C(36)	0.2490(2)	0.0596(2)	0.7500
O(37)	0.3316(2)	0.1685(2)	0.7500
N(38)	0.1836(2)	0.2588(2)	0.7500
O(39)	0.2464(2)	0.2929(2)	0.7500
O(40)	0.1180(2)	0.2902(2)	0.7500
N(41)	0.0234(2)	0.0365(2)	0.7500
O(42)	-0.0380(2)	0.0758(2)	0.7500
O(43)	0.0196(3)	-0.0309(2)	0.7500
N(44)	0.3186(2)	0.0093(2)	0.7500
O(45)	0.3048(2)	-0.0567(2)	0.7500
O(46)	0.3885(2)	0.0326(2)	0.7500

Table V. – Final atomic coordinates for **1**, Form **II**, room temperature.

Atom	x	y	z
N(1)	0.3345(1)	0.5030(3)	0.5901(2)
N(2)	0.2767(1)	0.7099(3)	0.4632(2)
C(1)	0.3917(1)	0.5816(3)	0.5888(3)
C(2)	0.4455(1)	0.5302(4)	0.6566(3)
C(3)	0.5001(1)	0.6007(4)	0.6457(4)
C(4)	0.5001(1)	0.7141(4)	0.5649(3)
C(5)	0.4454(1)	0.7693(3)	0.4935(3)
C(6)	0.4454(2)	0.8864(4)	0.4046(4)
C(7)	0.3930(2)	0.9399(5)	0.3375(5)
C(8)	0.3370(2)	0.8821(4)	0.3572(4)
C(9)	0.3345(1)	0.7681(3)	0.4400(3)
C(10)	0.3888(1)	0.7051(3)	0.5079(3)
C(11)	0.3329(2)	0.3713(4)	0.5073(5)
C(12)	0.3204(2)	0.4752(7)	0.7283(4)
C(13)	0.2325(2)	0.6887(7)	0.3409(4)
C(14)	0.2492(2)	0.7924(5)	0.5641(5)
C(31)	0.1385(1)	0.3691(3)	0.5544(3)
C(32)	0.1122(1)	0.2431(3)	0.4841(3)
C(33)	0.0527(1)	0.2030(3)	0.4767(3)
C(34)	0.0146(1)	0.2795(3)	0.5474(3)
C(35)	0.0358(1)	0.3938(3)	0.6259(3)
C(36)	0.0956(1)	0.4338(3)	0.6329(3)
O(37)	0.1890(1)	0.4177(3)	0.5426(3)
N(38)	0.1507(1)	0.1546(3)	0.4138(3)
O(39)	0.2051(1)	0.1463(3)	0.4599(3)
O(40)	0.1272(1)	0.0884(3)	0.3134(3)
N(41)	-0.0478(1)	0.2371(3)	0.5411(3)
O(42)	-0.0650(1)	0.1281(3)	0.4789(3)
O(43)	-0.0819(1)	0.3096(3)	0.5976(3)
N(44)	0.1152(1)	0.5520(3)	0.7217(3)
O(45)	0.0765(1)	0.6349(3)	0.7493(3)
O(46)	0.1696(1)	0.5653(4)	0.7658(4)

unchanged at room or low temperature, showing that some disorder is probably present. The value observed in the picrate salt (form **II**) is lower at 150 K than at room temperature, although both values are not significantly different in terms of the achieved precision. Figure 3 shows the Fourier difference synthesis in the plane defined by both nitrogen atoms and C(5) (room and low temperature) without including the hydrogen atom in the model. The maximum appears to be elongated in the N···N direction as in the PF_6^- salts (Fig. 4 in ref. 1), but while the electron density remains similar (or even slightly higher) in the N^+–H bond region, it drops in the H···N region when the temperature is decreased.

In compound **1** form **I**, the ions stack alternately along the *c* direction (Fig. 4a). The distance from the picrate plane to the naphthalene moiety is $c/2 = 3.48$ Å and agrees quite well with the van der Waals thickness of 3.4 Å for an aromatic ring, when considering the π interactions between the rings. In form **II**, both ions make an angle of 75.0(1)°. In compound **2**, the cations pack head-to-tail in piles along the *b* axis, allowing just partial overlapping of the naphthalene moiety. The distance between both naphthalene planes is 3.37(4) Å.

^{13}C and ^{15}N CPMAS NMR spectroscopy and X-ray structures of $DMANH^+$ salts

Besides salts **1** and **2**, natural abundance ^{13}C and ^{15}N-CPMAS-NMR spectra of the following $DMANH^+$ salts were measured because their X-ray structures are known: pentachlorophenolate **3**, squarate **4**, squarate with 4 water molecules in the crystal cell **5**, tetrazolate **6** and tetrafluoroborate **7**. Thiocyanate **8** data are from ref. 6 while the perchlorate **9** (X-ray structure unknown) was selected to test the predictive power of CPMAS NMR spectroscopy. All important results are summarized in Table X. Torsion angles affecting the methyl groups, τ_i, are defined as in Table IXa and Figure 2; $\tau_{av} = 1/4\,\Sigma\,|\tau_i|$, $\phi_1 = 1/2\,(|\tau_1| - |\tau_2|)$ and $\phi_2 = 1/2\,(|\tau_3| - |\tau_4|)$. The fact that $\tau_{av} = 63.5°$, and not 60° as for perfect sp^3 hybridization, is due to the nature of the hybridized atom (a neutral or a charged N instead of a sp^3 carbon), as well as to deviation of the N atoms from the naphthalene plane and to the non-planarity of the naphthalene skeleton. Although only **1I** strictly belongs to the **a** class ($\phi_1 = \phi_2 = 0$), we have considered that **4**, **5** (one independent molecule) and **6** also belong to this class.

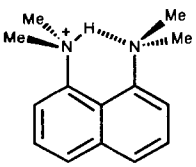

DMANH$^+$

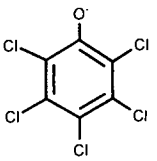

Pentachlorophenolate **3**

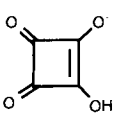

Squarates **4**, **5**

Tetrazolate **6**

BF_4^- **7**, SCN^- **8**, ClO_4^- **9**

A first observation is that the differences in the HBs (X-ray classes, **A**, **B** or **C**) does not arise from variations in the N···N distance (a shorter distance should correspond to the **B** class). This distance is always 2.55-2.59 Å long and even these small variations are unrelated to the nature of the HB system. The only structure belonging to class **C** (compound **5**) was refined with a 50:50 population disorder ($x = 0.5$) [27]; we will consider that 0.955 Å (the average value from the two molecules of compound **5**) is the "true" N–H bond length for structure **A**.

Since the N···N distance is the same, crystallographic class **B** may arise from class **C** ($K \approx 1$) if the difficulty in locating two "half-protons" results in finding the proton in the middle (**B** → 50% **C**′ + 50% **C**″). Moreover, those structures with "elongated" N–H bond lengths (**1II**, **1III**, **2**, **3**, **4**) may actually be class **C** compounds with $K \neq 1$. A step further is to assume that the longer the N–H bond length, the closer to 0.5 are the populations, **even if only the proton corresponding to the most populated position has been found**. A simple interpolation led to the following values: 1.08 Å → 85% of **C**′ ($K = 5$),

Table VI. – Final atomic coordinates for **1**, Form **II**, low temperature.

Atom	x	y	z
N(1)	0.3354(1)	0.5032(2)	0.5879(2)
N(2)	0.2773(1)	0.7144(2)	0.4612(2)
C(1)	0.3927(1)	0.5824(2)	0.5885(2)
C(2)	0.4468(1)	0.5304(3)	0.6595(2)
C(3)	0.5023(1)	0.5994(3)	0.6501(3)
C(4)	0.5021(1)	0.7146(3)	0.5674(3)
C(5)	0.4473(1)	0.7704(3)	0.4923(2)
C(6)	0.4479(1)	0.8863(3)	0.4009(3)
C(7)	0.3948(1)	0.9401(3)	0.3308(3)
C(8)	0.3378(1)	0.8841(3)	0.3501(3)
C(9)	0.3352(1)	0.7711(2)	0.4361(2)
C(10)	0.3902(1)	0.7072(2)	0.5064(2)
C(11)	0.3337(1)	0.3713(3)	0.5040(3)
C(12)	0.3208(1)	0.4747(3)	0.7286(3)
C(13)	0.2293(1)	0.7046(4)	0.3385(3)
C(14)	0.2539(1)	0.7938(3)	0.5722(3)
C(31)	0.1409(1)	0.3728(2)	0.5501(2)
C(32)	0.1149(1)	0.2434(2)	0.4824(2)
C(33)	0.0555(1)	0.2015(2)	0.4765(2)
C(34)	0.0170(1)	0.2792(2)	0.5456(2)
C(35)	0.0381(1)	0.3967(2)	0.6235(2)
C(36)	0.0980(1)	0.4381(2)	0.6297(2)
N(38)	0.1539(1)	0.1531(2)	0.4141(2)
O(39)	0.2091(1)	0.1472(2)	0.4628(2)
O(40)	0.1305(1)	0.0839(2)	0.3127(2)
N(41)	−0.0455(1)	0.2356(2)	0.5392(2)
O(42)	−0.0624(1)	0.1243(2)	0.4793(2)
O(43)	−0.0804(1)	0.3110(2)	0.5932(2)
N(44)	0.1176(1)	0.5588(2)	0.7176(2)
O(45)	0.0779(1)	0.6409(2)	0.7456(2)
O(46)	0.1724(1)	0.5741(2)	0.7625(2)

Table VII. – Final atomic coordinates for **2**, room temperature.

Atom	x	y	z
N(1)	−0.3043(4)	0.1676(5)	−0.2609(5)
N(2)	−0.3164(3)	0.3259(5)	−0.0298(5)
C(1)	−0.1830(4)	0.1901(6)	−0.1989(7)
C(2)	−0.1172(6)	0.1434(9)	−0.2838(10)
C(3)	−0.0013(7)	0.1562(10)	−0.2174(14)
C(4)	0.0462(6)	0.2088(8)	−0.0712(13)
C(5)	−0.0180(5)	0.2567(7)	0.0218(9)
C(6)	0.0311(6)	0.3079(8)	0.1786(11)
C(7)	−0.0300(7)	0.3571(10)	0.2645(11)
C(8)	−0.1457(6)	0.3629(9)	0.1966(9)
C(9)	−0.1968(4)	0.3127(6)	0.0457(6)
C(10)	−0.1360(4)	0.2527(6)	−0.0466(7)
C(11)	−0.3443(6)	−0.0070(8)	−0.2282(10)
C(12)	−0.3518(8)	0.2396(12)	−0.4359(9)
C(13)	−0.3853(7)	0.2518(11)	0.0814(9)
C(14)	−0.3416(6)	0.4989(8)	−0.0996(9)
P(1)	0.3127(1)	0.2472(2)	0.6473(2)
F(1)	0.2970(5)	0.1954(7)	0.8270(6)
F(2)	0.3888(5)	0.4020(7)	0.7019(7)
F(3)	0.2111(5)	0.3552(8)	0.5958(8)
F(4)	0.2327(6)	0.0979(8)	0.5933(9)
F(5)	0.3263(6)	0.3005(7)	0.4677(6)
F(6)	0.4144(5)	0.1420(9)	0.6994(10)

Table VIII. – Final atomic coordinates for **2**, low temperature.

Atom	x	y	z
N(1)	−0.3007(2)	0.1667(3)	−0.2579(3)
N(2)	−0.3201(2)	0.3185(3)	−0.0262(3)
C(1)	−0.1778(2)	0.1899(3)	−0.1911(4)
C(2)	−0.1082(3)	0.1464(4)	−0.2738(4)
C(3)	0.0092(3)	0.1604(4)	−0.2042(5)
C(4)	0.0538(3)	0.2129(4)	−0.0541(5)
C(5)	−0.0147(3)	0.2596(4)	0.0352(4)
C(6)	0.0310(3)	0.3105(4)	0.1942(4)
C(7)	−0.0354(3)	0.3564(5)	0.2791(4)
C(8)	−0.1524(3)	0.3588(4)	0.2055(4)
C(9)	−0.2000(2)	0.3092(3)	0.0544(3)
C(10)	−0.1345(2)	0.2526(3)	−0.0367(4)
C(11)	−0.3444(3)	−0.0142(4)	−0.2358(4)
C(12)	−0.3408(3)	0.2468(5)	−0.4329(4)
C(13)	−0.3947(3)	0.2360(4)	0.0790(4)
C(14)	−0.3448(3)	0.4954(4)	−0.0917(4)
P(1)	0.3139(1)	0.2518(1)	0.6451(1)
F(1)	0.2932(2)	0.1902(3)	0.8246(2)
F(2)	0.3818(2)	0.4211(3)	0.7082(3)
F(3)	0.2024(2)	0.3437(3)	0.5891(3)
F(4)	0.2457(3)	0.0848(3)	0.5849(3)
F(5)	0.3351(2)	0.3135(3)	0.4663(3)
F(6)	0.4281(2)	0.1647(3)	0.7051(3)

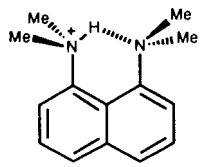

DMANH$^+$

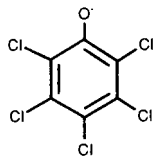

Pentachlorophenolate **3**

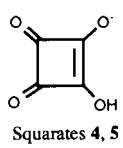

Squarates **4**, **5**

Tetrazolate **6**

BF_4^- **7**, SCN^- **8**, ClO_4^- **9**

A first observation is that the differences in the HBs (X-ray classes, **A**, **B** or **C**) does not arise from variations in the N···N distance (a shorter distance should correspond to the **B** class). This distance is always 2.55-2.59 Å long and even these small variations are unrelated to the nature of the HB system. The only structure belonging to class **C** (compound **5**) was refined with a 50:50 population disorder ($x = 0.5$) [27]; we will consider that 0.955 Å (the average value from the two molecules of compound **5**) is the "true" N–H bond length for structure **A**.

Since the N···N distance is the same, crystallographic class **B** may arise from class **C** ($K \approx 1$) if the difficulty in locating two "half-protons" results in finding the proton in the middle (**B** → 50% **C**′ + 50% **C**″). Moreover, those structures with "elongated" N–H bond lengths (**1II**, **1III**, **2**, **3**, **4**) may actually be class **C** compounds with $K \neq 1$. A step further is to assume that the longer the N–H bond length, the closer to 0.5 are the populations, **even if only the proton corresponding to the most populated position has been found**. A simple interpolation led to the following values: 1.08 Å → 85% of **C**′ ($K = 5$),

Table VI. – Final atomic coordinates for **1**, Form **II**, low temperature.

Atom	x	y	z
N(1)	0.3354(1)	0.5032(2)	0.5879(2)
N(2)	0.2773(1)	0.7144(2)	0.4612(2)
C(1)	0.3927(1)	0.5824(2)	0.5885(2)
C(2)	0.4468(1)	0.5304(3)	0.6595(2)
C(3)	0.5023(1)	0.5994(3)	0.6501(3)
C(4)	0.5021(1)	0.7146(3)	0.5674(3)
C(5)	0.4473(1)	0.7704(3)	0.4923(2)
C(6)	0.4479(1)	0.8863(3)	0.4009(3)
C(7)	0.3948(1)	0.9401(3)	0.3308(3)
C(8)	0.3378(1)	0.8841(3)	0.3501(3)
C(9)	0.3352(1)	0.7711(2)	0.4361(2)
C(10)	0.3902(1)	0.7072(2)	0.5064(2)
C(11)	0.3337(1)	0.3713(3)	0.5040(3)
C(12)	0.3208(1)	0.4747(3)	0.7286(3)
C(13)	0.2293(1)	0.7046(4)	0.3385(3)
C(14)	0.2539(1)	0.7938(3)	0.5722(3)
C(31)	0.1409(1)	0.3728(2)	0.5501(2)
C(32)	0.1149(1)	0.2434(2)	0.4824(2)
C(33)	0.0555(1)	0.2015(2)	0.4765(2)
C(34)	0.0170(1)	0.2792(2)	0.5456(2)
C(35)	0.0381(1)	0.3967(2)	0.6235(2)
C(36)	0.0980(1)	0.4381(2)	0.6297(2)
N(38)	0.1539(1)	0.1531(2)	0.4141(2)
O(39)	0.2091(1)	0.1472(2)	0.4628(2)
O(40)	0.1305(1)	0.0839(2)	0.3127(2)
N(41)	−0.0455(1)	0.2356(2)	0.5392(2)
O(42)	−0.0624(1)	0.1243(2)	0.4793(2)
O(43)	−0.0804(1)	0.3110(2)	0.5932(2)
N(44)	0.1176(1)	0.5588(2)	0.7176(2)
O(45)	0.0779(1)	0.6409(2)	0.7456(2)
O(46)	0.1724(1)	0.5741(2)	0.7625(2)

Table VII. – Final atomic coordinates for **2**, room temperature.

Atom	x	y	z
N(1)	−0.3043(4)	0.1676(5)	−0.2609(5)
N(2)	−0.3164(3)	0.3259(5)	−0.0298(5)
C(1)	−0.1830(4)	0.1901(6)	−0.1989(7)
C(2)	−0.1172(6)	0.1434(9)	−0.2838(10)
C(3)	−0.0013(7)	0.1562(10)	−0.2174(14)
C(4)	0.0462(6)	0.2088(8)	−0.0712(13)
C(5)	−0.0180(5)	0.2567(7)	0.0218(9)
C(6)	0.0311(6)	0.3079(8)	0.1786(11)
C(7)	−0.0300(7)	0.3571(10)	0.2645(11)
C(8)	−0.1457(6)	0.3629(9)	0.1966(9)
C(9)	−0.1968(4)	0.3127(6)	0.0457(6)
C(10)	−0.1360(4)	0.2527(6)	−0.0466(7)
C(11)	−0.3443(6)	−0.0070(8)	−0.2282(10)
C(12)	−0.3518(8)	0.2396(12)	−0.4359(9)
C(13)	−0.3853(7)	0.2518(11)	0.0814(9)
C(14)	−0.3416(6)	0.4989(8)	−0.0996(9)
P(1)	0.3127(1)	0.2472(2)	0.6473(2)
F(1)	0.2970(5)	0.1954(7)	0.8270(6)
F(2)	0.3888(5)	0.4020(7)	0.7019(7)
F(3)	0.2111(5)	0.3552(8)	0.5958(8)
F(4)	0.2327(6)	0.0979(8)	0.5933(9)
F(5)	0.3263(6)	0.3005(7)	0.4677(6)
F(6)	0.4144(5)	0.1420(9)	0.6994(10)

Table VIII. – Final atomic coordinates for **2**, low temperature.

Atom	x	y	z
N(1)	−0.3007(2)	0.1667(3)	−0.2579(3)
N(2)	−0.3201(2)	0.3185(3)	−0.0262(3)
C(1)	−0.1778(2)	0.1899(3)	−0.1911(4)
C(2)	−0.1082(3)	0.1464(4)	−0.2738(4)
C(3)	0.0092(3)	0.1604(4)	−0.2042(5)
C(4)	0.0538(3)	0.2129(4)	−0.0541(5)
C(5)	−0.0147(3)	0.2596(4)	0.0352(4)
C(6)	0.0310(3)	0.3105(4)	0.1942(4)
C(7)	−0.0354(3)	0.3564(5)	0.2791(4)
C(8)	−0.1524(3)	0.3588(4)	0.2055(4)
C(9)	−0.2000(2)	0.3092(3)	0.0544(3)
C(10)	−0.1345(2)	0.2526(3)	−0.0367(4)
C(11)	−0.3444(3)	−0.0142(4)	−0.2358(4)
C(12)	−0.3408(3)	0.2468(5)	−0.4329(4)
C(13)	−0.3947(3)	0.2360(4)	0.0790(4)
C(14)	−0.3448(3)	0.4954(4)	−0.0917(4)
P(1)	0.3139(1)	0.2518(1)	0.6451(1)
F(1)	0.2932(2)	0.1902(3)	0.8246(2)
F(2)	0.3818(2)	0.4211(3)	0.7082(3)
F(3)	0.2024(2)	0.3437(3)	0.5891(3)
F(4)	0.2457(3)	0.0848(3)	0.5849(3)
F(5)	0.3351(2)	0.3135(3)	0.4663(3)
F(6)	0.4281(2)	0.1647(3)	0.7051(3)

Table IXb. – Selected geometrical parameters for the picrate anion. LT indicates data at low temperature (distances in Å, torsion angles in °).

Form	I	II (LT)
C(31)–C(32)	1.470(5)	1.465(3)
C(31)–C(36)	1.464(5)	1.461(3)
C(31)–O(37)	1.239(5)	1.238(3)
C(32)–(C33)	1.358(6)	1.366(3)
C(32)–N(38)	1.453(5)	1.455(3)
C(33)–C(34)	1.389(6)	1.385(3)
C(34)–C(35)	1.382(6)	1.386(3)
C(34)–N(41)	1.435(6)	1.436(3)
C(35)–C(36)	1.360(5)	1.376(3)
C(36)–N(44)	1.454(5)	1.454(3)
N(38)–O(39)	1.195(5)	1.236(3)
N(38)–O(40)	1.208(5)	1.231(3)
N(41)–O(42)	1.226(5)	1.234(3)
N(41)–O(44)	1.230(5)	1.235(3)
N(44)–O(45)	1.222(4)	1.239(3)
N(44)–O(46)	1.212(5)	1.229(3)
C(36)–C(31)–O(37)	124.3(3)	124.8(2)
C(32)–C(31)–O(37)	124.8(3)	124.3(2)
C(32)–C(31)–C(36)	110.9(3)	110.8(2)
C(31)–C(32)–N(38)	119.9(3)	118.8(2)
C(31)–C(32)–C(33)	124.7(3)	124.4(2)
C(33)–C(32)–N(38)	115.4(3)	116.8(2)
C(32)–C(33)–C(34)	119.3(3)	119.4(2)
C(33)–C(34)–N(41)	119.2(3)	119.5(2)
C(33)–C(34)–C(35)	120.9(3)	121.2(2)
C(35)–C(34)–N(41)	119.9(3)	119.3(2)
C(34)–C(35)–C(36)	120.0(3)	119.1(2)
C(35)–C(36)–C(31)	124.2(3)	124.2(2)
C(35)–C(36)–N(44)	115.4(3)	116.2(2)
C(31)–C(36)–N(44)	120.4(3)	119.5(2)
C(31)–C(32)–N(38)–O(39)	0	32.3(3)
C(33)–C(34)–N(41)–O(42)	0	4.6(3)
C(31)–C(36)–N(44)–O(46)	0	–25.3(3)

Tables XI summarizes the crystallographic and NMR information on protonated sponges. If the "conformational class" **a** or **b**, is in general correct (the only exception being the squarate **4**), the description of the $(NHN)^+$ IMHB presents several difficulties.

Picrate **1I**, according to crystallography, belongs to the **Aa** or perhaps to the **Ca** class ($K \approx 2$), but according to CPMAS NMR it belongs to the $\mathbf{E_1a}$ or $\mathbf{E_2a}$ classes ($K = 1$). Consequently, even assuming the **Ca** structure, there is an inconsistency because the X-ray results clearly exclude a 50:50 population. The only possible explanation is a lack of resolution, i.e. that the chemical shift differences in both ^{13}C and ^{15}N CPMAS (see comment (ii) in the discussion of Table I) are not large enough. Crystallographically, picrate **1II** belongs to the **Ab** or perhaps to the **Cb** class ($K \approx 3.5$) and spectroscopically to the **Fb** or **Gb** classes, which is consistent (see Table I for correspondences) assuming the **Cb** hypothesis. In the case of the hexafluorophosphate salt **2** it is also necessary to assume a **Cb** structure ($K \approx 2$) to be consistent with the NMR result ($\mathbf{E_1b}$).

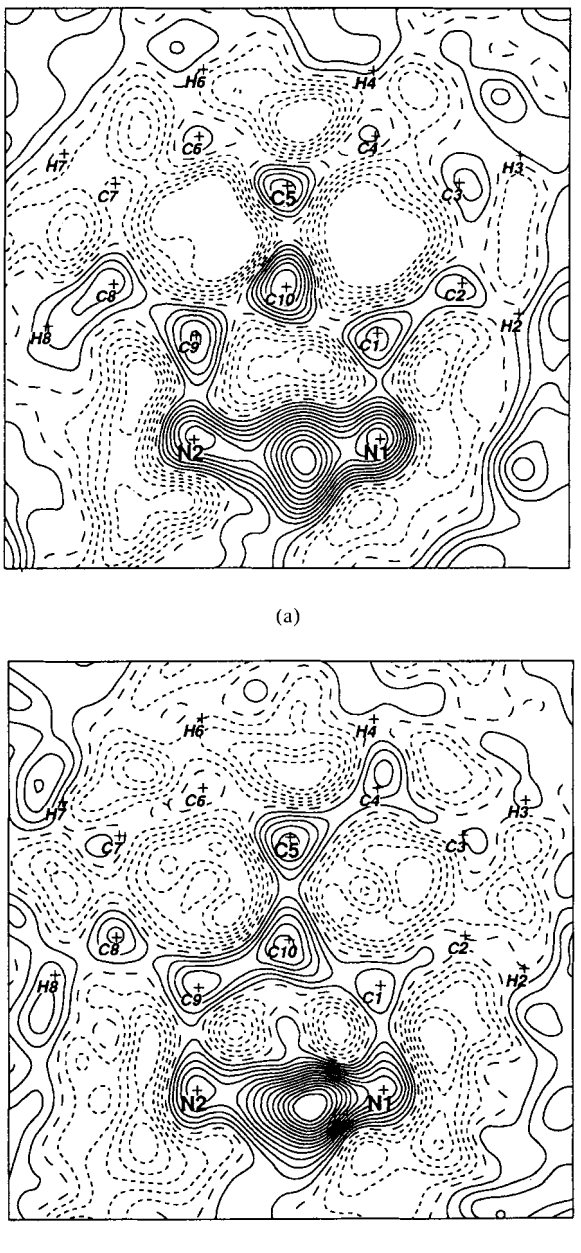

Figure 3. – Fourier difference synthesis in the plane defined by N(1), N(2) and C(5) for compound **III** after removing the proton from the model: (a) at room and (b) at low temperature. Lines indicate electron density in steps of 0.04 e $Å^{-3}$.

Compound **3** shows a perfect agreement between X-ray crystallography (assuming a **Cb** class with $K \approx 3.5$) and CPMAS NMR ($\mathbf{D_1b}$ or **Gb**). There are two squarates, the anhydrous form **4** (**Ab** or **Cb** with $K = 5$) and the tetra-hydrate **5** (**Aa + Ab**); for this last one, both independent molecules have very short N–H bonds

indicative of pure **A** class. We have only studied the anhydrous variety (m.p. 210-4 °C, no m.p. reported in the crystallographic papers [26, 27]); in this case there is an inconsistency between crystallography (class **b**) and ^{13}C CPMAS NMR (only one methyl group, class **a**); the only possible explanation is a lack of resolution. The tetrazolate **6** (**Ba** or **Ca** with $K = 1$) also shows the consistency of both techniques if the structure is either **Ba** ($\mathbf{E_2a}$) or **Ca** with $K = 1$ ($\mathbf{E_1a}$).

Although the **Bb** or **Cb** with $K = 1$ classes of tetrafloroborate **7** and thiocyanate **8** are other examples of consistency (we suppose that the $DMANH^+$ cation of **8**, if recorded, will show only one ^{15}N signal) as well as of the inability to choose between **Bb** and **Cb**, there is an

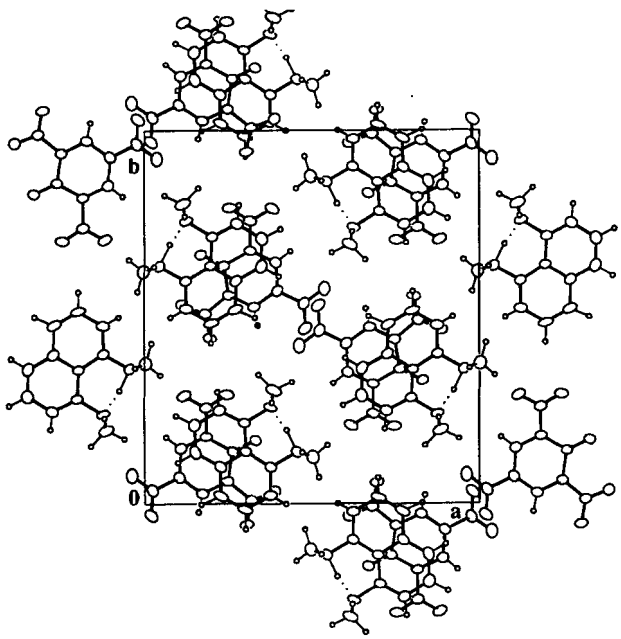

(4a)

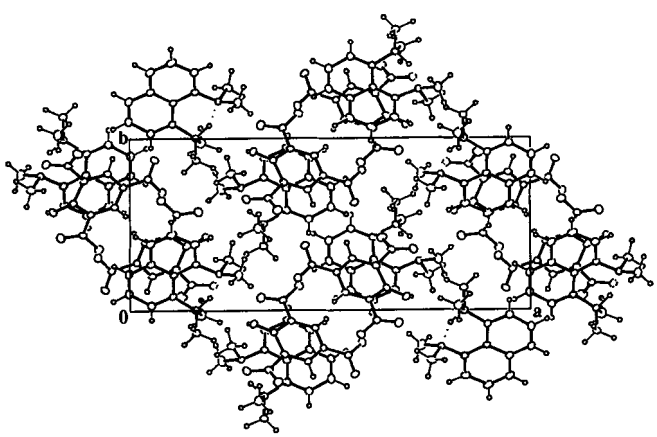

(4b)

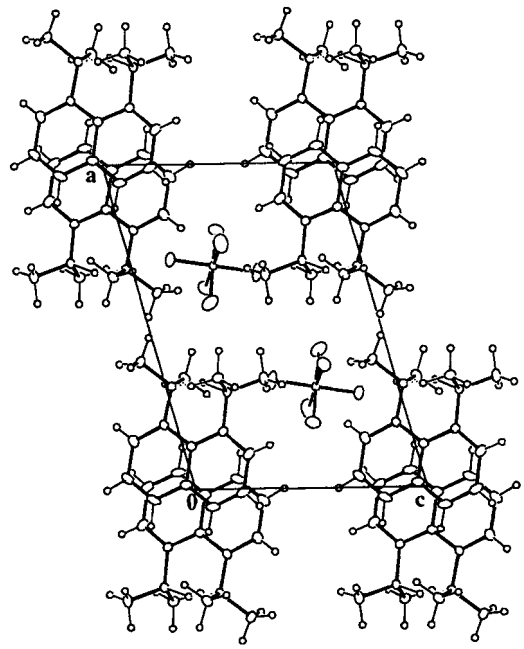

(4c)

Figure 4. – Crystal packing of **1** down the *c* axis: (a and b) form **I** and **II**. (c) Same for **2** down the *b* axis.

ESCA result [29] indicating that both nitrogen atoms of **7** are non-equivalent, i.e. that it belongs to the **Cb** class. According to those findings, the perchlorate **9** (2 Me, 1N) should belong to the **Bb** or **Cb** ($K = 1$) classes (see in Table V the similarity of the chemical shifts of compounds **7** and **9**).

Conclusions

The first conclusion of this study is the acceptable consistency of the two techniques the most often used for solid-state studies of organic compounds: X-ray crystallography and CPMAS NMR spectroscopy. The second is that they are complementary, in particular NMR is able to detect proton disorder in the $(NHN)^+$ IMHB. Moreover, since the N···N distance in compounds **4**, **6**, **7** and **8** is the same as for other $DMANH^+$ cations, we propose the working hypothesis that these compounds do not belong to the **B** class but to the **C** class, even if the proton refined position is in the center of the IMHB. This agrees with the conclusion of Hibbert and Emsley [30] that protonated proton sponges have HBs of moderate strength with a double minimum potential, with the conclusion of Toppet et al. [31] that the $DMANH^+$ cation in solution includes two symmetrically situated wells between which fast proton migration occurs, and also with the ESCA study of compound **7** [29].

Table IXb. – Selected geometrical parameters for the picrate anion. LT indicates data at low temperature (distances in Å, torsion angles in °).

Form	I	II (LT)
C(31)–C(32)	1.470(5)	1.465(3)
C(31)–C(36)	1.464(5)	1.461(3)
C(31)–O(37)	1.239(5)	1.238(3)
C(32)–(C33)	1.358(6)	1.366(3)
C(32)–N(38)	1.453(5)	1.455(3)
C(33)–C(34)	1.389(6)	1.385(3)
C(34)–C(35)	1.382(6)	1.386(3)
C(34)–N(41)	1.435(6)	1.436(3)
C(35)–C(36)	1.360(5)	1.376(3)
C(36)–N(44)	1.454(5)	1.454(3)
N(38)–O(39)	1.195(5)	1.236(3)
N(38)–O(40)	1.208(5)	1.231(3)
N(41)–O(42)	1.226(5)	1.234(3)
N(41)–O(44)	1.230(5)	1.235(3)
N(44)–O(45)	1.222(4)	1.239(3)
N(44)–O(46)	1.212(5)	1.229(3)
C(36)–C(31)–O(37)	124.3(3)	124.8(2)
C(32)–C(31)–O(37)	124.8(3)	124.3(2)
C(32)–C(31)–C(36)	110.9(3)	110.8(2)
C(31)–C(32)–N(38)	119.9(3)	118.8(2)
C(31)–C(32)–C(33)	124.7(3)	124.4(2)
C(33)–C(32)–N(38)	115.4(3)	116.8(2)
C(32)–C(33)–C(34)	119.3(3)	119.4(2)
C(33)–C(34)–N(41)	119.2(3)	119.5(2)
C(33)–C(34)–C(35)	120.9(3)	121.2(2)
C(35)–C(34)–N(41)	119.9(3)	119.3(2)
C(34)–C(35)–C(36)	120.0(3)	119.1(2)
C(35)–C(36)–C(31)	124.2(3)	124.2(2)
C(35)–C(36)–N(44)	115.4(3)	116.2(2)
C(31)–C(36)–N(44)	120.4(3)	119.5(2)
C(31)–C(32)–N(38)–O(39)	0	32.3(3)
C(33)–C(34)–N(41)–O(42)	0	4.6(3)
C(31)–C(36)–N(44)–O(46)	0	–25.3(3)

Tables XI summarizes the crystallographic and NMR information on protonated sponges. If the "conformational class" **a** or **b**, is in general correct (the only exception being the squarate **4**), the description of the $(NHN)^+$ IMHB presents several difficulties.

Picrate **1II**, according to crystallography, belongs to the **Aa** or perhaps to the **Ca** class ($K \approx 2$), but according to CPMAS NMR it belongs to the $\mathbf{E_1a}$ or $\mathbf{E_2a}$ classes ($K = 1$). Consequently, even assuming the **Ca** structure, there is an inconsistency because the X-ray results clearly exclude a 50:50 population. The only possible explanation is a lack of resolution, i.e. that the chemical shift differences in both ^{13}C and ^{15}N CPMAS (see comment (ii) in the discussion of Table I) are not large enough. Crystallographically, picrate **1III** belongs to the **Ab** or perhaps to the **Cb** class ($K \approx 3.5$) and spectroscopically to the **Fb** or **Gb** classes, which is consistent (see Table I for correspondences) assuming the **Cb** hypothesis. In the case of the hexafluorophosphate salt **2** it is also necessary to assume a **Cb** structure ($K \approx 2$) to be consistent with the NMR result ($\mathbf{E_1b}$).

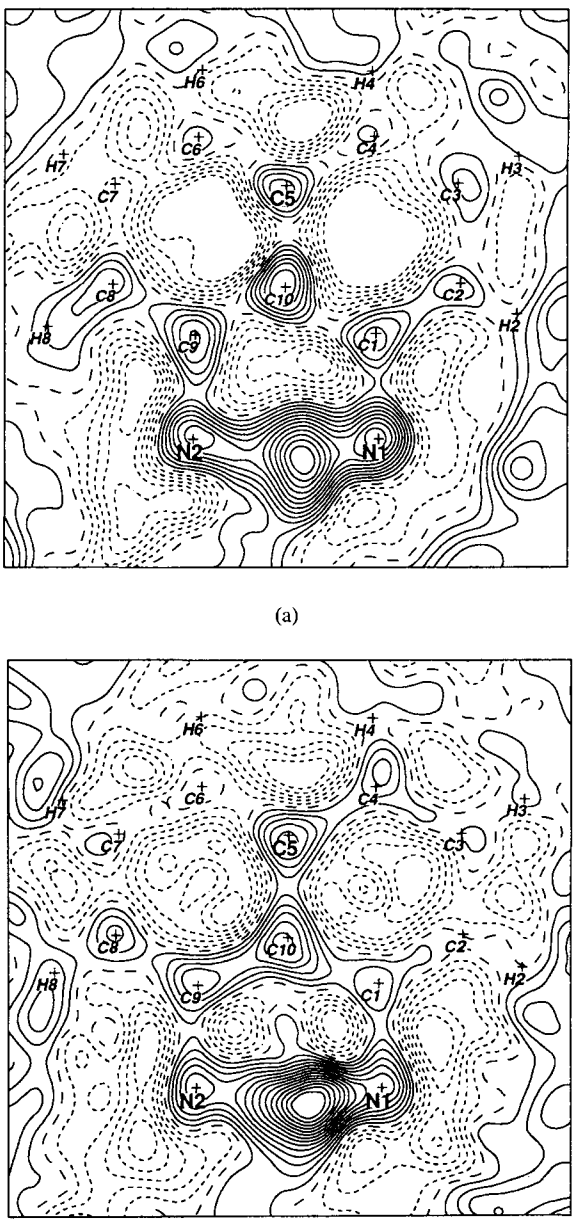

Figure 3. – Fourier difference synthesis in the plane defined by N(1), N(2) and C(5) for compound **1III** after removing the proton from the model: (a) at room and (b) at low temperature. Lines indicate electron density in steps of 0.04 e $Å^{-3}$.

Compound **3** shows a perfect agreement between X-ray crystallography (assuming a **Cb** class with $K \approx 3.5$) and CPMAS NMR ($\mathbf{D_1b}$ or **Gb**). There are two squarates, the anhydrous form **4** (**Ab** or **Cb** with $K = 5$) and the tetra-hydrate **5** (**Aa** + **Ab**); for this last one, both independent molecules have very short N–H bonds

Table X. – CPMAS NMR *vs* crystallography in $DMANH^+$ X^- complexes (distances in Å and torsion angles in °).

Anion	^{13}C NMR (no of Me signals)	^{15}N NMR (no of N signals)	X-ray crystallography								
			N–H	N···N	Me torsions							Class	Temp. and ref.
					τ_1	τ_2	τ_3	τ_4	τ_{av}	ϕ_1	ϕ_2		
Picrate **1** form **I**	1	1	1.19	2.57	−63.9	63.9	63.6	−63.6	63.8	0.0	0.0	**Aa**	This work
Picrate **1** form **II**	4	4 (1:1:2)	1.11	2.58	−70.6	57.1	41.5	−84.2	63.4	6.8	21.4	**Ab**	This work
PF_6^- **2**	2	1	1.19	2.57	73.6	−53.5	−52.4	74.1	63.4	10.0	10.9	**Ab**	This work
$C_6Cl_5O^-$ **3**	4 (1:1:2)	2	1.11	2.55	66.4	−60.9	−68.7	57.8	63.4[a]	2.8[a]	5.4[a]	**Ab**	100 K [24]
Squarate **4**	1	1	1.08	2.58	70.2	−56.7	−65.3	61.1	63.3	6.8	2.1	**Ab**	150 K [25]
Squarate, 4 H_2O **5**[b]	–	–	0.97	2.59	62.4	−64.0	−62.4	64.0	63.2	0.8	0.8	**Aa**	100 K [26]
			0.94	2.57	58.5	−68.2	−58.5	68.2	63.4	4.8	4.8	**Ab**	100 K [26]
Tetrazolate **6**	1	1	1.31	2.57	64.8	−62.5	−64.8	62.5	63.6	1.2	1.2	**Ba**	RT [27]
BF_4^- **7**	2	1	1.31	2.56	−75.6	50.6	51.1	−76.7	63.5	12.5	12.8	**Bb**	RT [28]
SCN^- **8**	2[6]	–	1.32	2.57	73.8	−53.1	−73.8	53.1	63.5	10.4	10.4	**Bb**	188 K [4]
ClO_4^- **9**	2	1	**Unknown**										
AM1			1.07	2.72	62.2	−62.2	−64.2	64.2	63.2	0.0	0.0	**Aa**	1
6-31G			1.05	2.64	63.9	−65.0	−65.0	63.9	64.4	0.6	0.6	**Aa**	5

[a] At RT = 63.2°, 2.8°, 6.4°. [b] Two independent molecules.

Table XI. – Relationship between crystallography and CPMAS NMR (experimental results).

	X-ray crystallography		^{13}C and ^{15}N CPMAS NMR
	Exp.	Possible	
Picrate **1** form **I**	**Aa**	**Ca** ($K \neq 1$)	**E_1a, E_2a**
Picrate **1** form **II**	**Ab**	**Cb** ($K \neq 1$)	**Fb, Gb**
PF_6^- **2**	**Ab**	**Cb** ($K \neq 1$)	**E_1b, E_2b**
$C_6Cl_5O^-$ **3**	**Ab**	**Cb** ($K \neq 1$)	**D_1b, D_2b, Ga, Gb**
Squarate **4**	**Ab**	**Cb** ($K \neq 1$)	**E_1a, E_2a**
Squarate, 4 H_2O **5**	**Ab + Ab**	**Aa + Ab**	**Unknown**
Tetrazolate **6**	**Ba**	**Ca** ($K = 1$)	**E_1a, E_2a**
BF_4^- **7**	**Bb**	**Cb** ($K = 1$)	**E_1b, E_2b**
SCN^- **8**	**Bb**	**Cb** ($K = 1$)	**E_1b, E_2b**[a]
ClO_4^- **9**		**Unknown**	**E_1b, E_2b**

[a] Since the ^{15}N CPMAS NMR was not reported, other solutions are possible: **D_1a**, **D_2a** and **Fa**.

In the case of NH-pyrazoles proton transfer, ^{15}N CPMAS chemical shifts and ^1H–^2H isotope effects were well-suited for determining the activation energy and the mechanism of the proton transfer [13, 32]; the reason is that the chemical shifts of the nitrogen atoms differ by about 60-80 ppm [12]. For the $DMANH^+$ cation, the difference in chemical shifts between NMe_2 and NMe_2H^+ is quite small, less than 10 ppm (see Table V); consequently, chemical shifts would not be the best method for studying proton transfer in these compounds by CPMAS NMR.

Acknowledgments

Thanks are given to the DGICYT of Spain for financial support (Projects number PB93-0125 and PB93-0197-C02) and to the EU for a HC&M network (No. CHRX CT 940582). One of us (C.L.) thanks the *Comunidad de Madrid* for a grant during her stay at the Freie Universität of Berlin. Another us (H.H.L.) thanks the Fonds der Chemischen Industrie, Frankfurt, for financial support.

References

[1] Llamas-Saiz A. L., Foces-Foces C., Elguero J., *J. Mol. Struct.*, 1994, **328**, 297.

[2] Dega-Szafran Z., Nowak-Wydra B., Szafran M., *Magn. Reson. Chem.*, 1993, **31**, 726.

[3] Klimkiewicz J., Stefaniak L., Brzezinski B., Grech E., Kuroki S., Ando I., Webb G. A., *J. Mol. Struct.*, 1994, **323**, 193.

[4] Bartoszak E., Jaskólski M., Grech E., Gustafsson T., Olovson I., *Acta Crystallogr. Sect. B*, 1994, **50**, 358.

[5] Platts A., Howard S. T., Wozniak K., *J. Org. Chem.*, 1994, **59**, 4647.

[6] Wozniak K., He H., Klinowski J., Grech E., *J. Phys. Chem.*, 1995, **99**, 1403.

[7] Etter M. C., Hoye R. C., Vojta G. M., *Cryst. Rev.*, 1988, **1**, 281.

[8] Monge M. A., Puebla E. G., Elguero J., Toiron C., Meutermans W., Sobrados I., *Spectrochim. Acta, Part A*, 1994, **50**, 727.

[9] Claramunt R. M., Dotor J., Sanz D., Foces-Foces C., Llamas-Saiz A. L., Elguero J., Flammang R., Morizur J. P., Chapon E., Tortajada J., *Helv. Chim. Acta*, 1994, **77**, 121.

[10] Grech E., Stefaniak L., Ando I., Yoshimizu H., Webb G. A., *Bull. Chem. Soc. Jpn.*, 1991, **64**, 3761.

[11] Grech E., Stefaniak L., Ando I., Yoshimizu H., Webb G. A., Sobczyk L., *Bull. Chem. Soc. Jpn.*, 1990, **63**, 2716.

[12] Aguilar-Parrilla F., Männle F., Limbach H.-H., Elguero J., Jagerovic N., *Magn. Res. Chem.*, 1994, **32**, 699.

[13] Aguilar-Parrilla F., Limbach H.-H., Foces-Foces C., Cano F. H., Jagerovic N., Elguero J., *J. Org. Chem.*, 1995, **60**, 1965.

[14] Srinivasan P. R., Lichter R. L., *J. Magn. Res.*, 1977, **28**, 227.

[15] Witanowski M., Stefaniak L., Szymanski S., Januszewski H., *J. Magn. Res.*, 1977, **28**, 217.

[16] Nelson J. H., Takach N. E., Henry R. A., Moore D. W., Tolles W. M., Gray G. A., *Magn. Res. Chem.*, 1986, **24**, 984.

[17] Altomare A., Burla M. C., Camalli M., Cascarano G., Giacovazzo C., Guagliardi A., Polidori G., SIR92, *J. Appl. Crystallogr.*, 1994, 435.

[18] Walker N., Stuart D., *Acta Crystallogr. Sect. A*, 1983, **39**, 158.

[19] Stewart J. M., Machin P. A., Dickinson C. W., Ammon H. L., Heck H., Flack H., *The X-Ray System*, 1976, Technical report TR-446. Computer Science Center, Univ. of Maryland.

[20] *International Tables for X-Ray Crystallography*, Birmingham, Kynoch Press, England, 1974, vol. IV.

[21] Hall S. R., Flack H. D., Stewart J. M., *Xtal3.2*, 1994, Eds. Univ. of Western Australia. Lamb: Perth.

[22] Abrahams S. C., Keve E. T., *Acta Cyrstallogr. Sect. A*, 1971, **27**, 157.

[23] Cano F. H., Foces-Foces C., Garcia-Blanco S., *J. Cryst. Mol. Struct.*, 1979, 9, 107.

[24] Kanters J. A., Ter Horst E. T., Kroon J., Grech E., *Acta Crystallogr. Sect. C*, 1992, **48**, 328.

[25] Wozniak K., Schouten A., Kroon J., Grech E., *Acta Crystallogr. Sect. C*, 1991, **47**, 807.

[26] Kanters J. A., Schouten A., Kroon J., Grech E., *Acta Crystallogr. Sect. C*, 1992, **48**, 1254.

[27] Glowiak T., Malarski Z., Sobczyk L., Grech E., *J. Mol. Struct.*, 1992, **270**, 441.

[28] Wozniak K., Krygowski T. M., Kariuki B., Jones W., Grech E., *J. Mol. Struct.*, 1990, **240**, 111.

[29] Hasselbach E., Henriksson A., Jachimowicz F., Wirz J., *Helv. Chim. Acta*, 1972, **55**, 1757.

[30] Hibbert F., Emsley J., *Adv. Phys. Org. Chem.*, 1990, **26**, 255.

[31] Toppet S., Platteborze K., Zeegers-Huyskens T., *J. Chem. Soc., Perkin Trans 2*, 1995, 831.

[32] Aguilar-Parrilla F., Scherer G., Limbach H.-H., Foces-Foces C., Cano F. H., Smith J. A. S., Toiron C., Elguero J., *J. Am. Chem. Soc.*, 1992, **114**, 9657.